International Journal of Mechanical and Production Engineering Research and Development (IJMPERD)
ISSN(P): 2249-6890; ISSN(E): 2249-8001
Vol. 5, Issue 1, Feb 2015, 83-104

OPTIMIZING THE MECHANICAL PROPERTIES OF TI-6AL-4V CASTINGS

REHAM REDA[1], ABDEL-HAMID HUSSEIN[2], ADEL NOFAL[3] & EL-SAYED M. EL-BANNA[4]

[1,3]Central Metallurgical R & D Institute, Helwan, Egypt

[2,4]Faculty of Engineering, Cairo University, Egypt

ABSTRACT

The use of Ti-alloys in the as-cast condition leads to a considerable savings in the manufacturing costs. This study aimed at optimizing the mechanical properties of Ti-6Al-4V castings through studying the effect of different pre-designed heat treatment cycles on the microstructure and mechanical properties of cast Ti-6Al-4V alloy. The design and selection of the heat treatment cycles was made after determination of the transformation temperatures of the alloy, β-transus (T_β) and martensite start transformation (Ms) temperatures. The alloy was characterized before and after heat treatments using microstructural investigation in addition to tensile and Charpy impact toughness tests. The fracture surfaces of the broken impact samples were investigated using Scanning Electron Microscope (SEM). Finally, the relation between the heat treatment, microstructure and mechanical properties of Ti-6Al-4V cast alloy was established and the optimum heat treatment cycle that optimized the mechanical properties was selected.

KEYWORDS: Ti-6Al-4V Castings, Single/Duplex Stage Heat Treatment, Microstructure, Retained β-Phase, Tensile Properties, Charpy Impact Toughness, Fracture Surface

INTRODUCTION

Ti-6Al-4V is the workhorse of the titanium industry; it accounts for about 60% of the total titanium production. The existence of the α/β transformation means that a variety of microstructures and property combinations can be achieved in the alloy through heat treatment, thus permitting the adaptation of properties to new applications.[1-4] Figure 1 presents schematic binary phase diagram of Ti-6Al-4V alloy. This alloy has an excellent combination of strength, toughness and good corrosion resistance and finds uses in aerospace applications, pressure vessels, aircraft-turbine and compressor blades and surgical implants.[4,5] Although in use for a number of years, Ti-6Al-4V alloy still attracts the attention of researchers from both fundamental and practical point of view.[5] Due to the high cost of titanium, e.g. material and processing costs, the use of net-shape or near-net-shape technologies receives an increasing interest considering the large cost saving potential of this technology in manufacturing parts of complex shapes.[2,5-7] Casting technologies enable the manufacture of complex shapes and large parts.[2,4-7]

A deep understanding of the phase transformations and microstructural modifications occurring during processing, e.g. heat treatment, is thus required to allow the improvement of the mechanical performances. ***The objective*** of this paper was to optimize the mechanical properties of Ti-6Al-4V castings through the following procedure: (i) studying the effect of different pre-designed heat treatment cycles on the microstructure and mechanical properties, and (ii) selecting the best heat

treatment cycle that optimizes the properties after establishing a relation between the heat treatment, microstructure and mechanical properties of Ti-6Al-4V cast alloy.

EXPERIMENTAL WORK

Materials and Methods

The material used in this study was cast Ti-6Al-4V alloy cylindrical ingot of 120mm diameter and 200mm height manufactured by Baoji intelle metals Co., Ltd., China.

Determination of the Phase Transformation Temperatures

Beta transus temperature (Tβ) is measured using heat-flux differential scanning calorimetry. Samples were heated to 1200°C with heating rate of 10°C/min, allowed to equilibrate for 2 minutes, and then cooled with rate of 50°C/min. Heat taken up or given off during the analysis was plotted against temperature during cooling/heating. From this test, β-transus transformation temperature was determined on heating and cooling.

Martensitic transformation start temperature (Ms) is measured using data logger thermal Analysis device with a thermocouple type-K. The sample with the connected thermocouple was put in the heat treatment furnace and heated up by 10˚C/min to 1050˚C (i.e. 63˚C above Tβ, as verified by DSC heating curve at the same heating rate) and held for 10 min, then quenched in water. Variations in the temperature (˚C) with time were recorded and the cooling curve was drawn then analyzed in order to estimate the martensitic transformation start temperature (Ms).

Heat Treatment

This work involved 9 designed heat treatment cycles. Three of them were called single stage heat treatment (SSHT) cycles and the other six were called duplex stage heat treatment (DSHT) cycles as shown in Figure 2 and Figure 3, respectively. The heat treatment cycles performed in this study were selected after determining the transformation temperature of the alloy, i.e. T_β and M_s. The results show that T_β and M_s are 987°C and 830°C, respectively, as will be illustrated in Sec.3.1.1. SSHT temperatures and temperatures of the first step of DSHT were selected to be below T_β to avoid grain coarsening and formation of high percent of the brittle martensite (α') phase on quenching. Programmable furnace with a controlled atmosphere (argon environment) was used for all heat treatment cycles.

Single Stage Heat Treatment (SSHT)

In single stage heat treatment (SSHT), the samples were heated up to different temperatures in α+β range (900°C, 935°C, 980°C) with heating rate 10°C/min. The samples were isothermally held for 10min, followed by water quenching, as shown in Figure 2.

Duplex Stage Heat Treatment (DSHT)

The duplex stage heat treatment (DSHT) involved heating samples up the same temperatures of the SSHT temperatures (900°C, 935°C, 980°C) with heating rate 10°C/min. and isothermally held for 10min, followed by the furnace cooling, with cooling rate 50°C/min, to lower temperatures (600°C and 700°C), and isothermally held for 30min. Finally specimens were water quenched down to room temperature, as shown in Figure 3.

Testing and Examinations

Microstructure Investigation

The as-cast and heat-treated specimens were prepared by standard metallographic techniques which consist of polishing and etching in an etchant composed of 10% HNO_3, 5% HF, and 85% distilled water. After etching, the specimens were investigated by an optical microscope, scanning electron microscope (SEM) and energy-dispersive spectrometry (EDS). The volume fractions of the different phases were measured using an image analyzer and X-ray diffraction. X-ray diffraction analysis with CuKα irradiation was used for microstructural characterization. X-ray diffraction measurements were made using the angle (2θ) from 34° to 42° by step 0.02°.

Mechanical Testing

Tensile Test

Tensile specimens of 130mm long with a gauge length of 30mm and gauge diameter of 6mm according to ASTM E8 were prepared from the as-cast material. Uniaxial tensile tests were carried out at room temperature at a strain rate of 0.5mm/min.

Charpy Impact Test

Standard Charpy V-notch impact specimens were machined in accordance with ASTM E23 standard specification. Charpy impact tests were done using a 150-J maximum capacity machine at room temperature. After impact testing, fracture surfaces were observed carefully by SEM to investigate the fracture mode and crack propagation behavior.

RESULTS AND DISCUSSIONS

Transformation and Microstructural Evaluation in Ti-6Al-4V Alloy

When Ti-6Al-4V α+β Ti-alloy is heated to α+β-region, held then cooled, the alloy exhibits various transformed microstructures depending on the cooling rate. When cooling rate is high, a martensitic structure or fine Widmanstatten structure (a mixture of the grain boundary α-phase and side-plate α-phase) is formed. When the cooling rate is lower, a coarse Widmanstatten structure is formed, as reported in many papers.[6-12]

Phase Transformation of Ti-6Al-4V Alloy

Relatively little attention has been paid to the solid→solid phase transformations occurring upon heating, which is usually the first step of treatment and processing. In the present work, the α/β transformations during continuous heating and cooling processes have been studied. Differential scanning calorimetry (DSC) is an experimental technique used for investigating phase transformations and reactions which involve heat absorption and/or heat release. The temperatures of the transformation can be measured from the onset and offset points of the peak.[13,14]

Differential scanning calorimetry (DSC) heating and cooling curves for Ti-6Al-4V alloy used in this study are shown in Figure 4. It is reported that[8,15] α→β transformation starts during heating from room temperature. As the temperature increases, β-phase fraction increases and becomes progressively less constrained by the α-phase and its lattice expands progressively up to reach β-transus temperature (Tβ) where the transformation is complete, as illustrated in Ti-6Al-4V alloy

phase diagram presented in Figure 1 DSC heating curve for Ti-6Al-4V alloy used in this study shows one endothermic DSC peak between the onset and the offset points of the α→β phase transformation, which represents Tβ. In accordance with DSC heating curve, α→β transformation is completed at about 987°C, as shown in Figure 4a. This result conforms to previous studies.[1,5,8,11,13,14,16,17] Sha and Guo[13] found that there are two endothermic DSC peaks between the onset and the offset points of the α→β phase transformation during heating. These are considered as two procedures correlated to α+β→β transformation. This difference between our results and results reported by Sha and Guo[13] is attributed to the difference in the starting microstructure. In this study, the starting microstructure was in the as-cast condition while the later[13] used the microstructure in the wrought condition. Sha and Guo[13] reported that these two peaks correspond to the transformation from the α in the transformed β-phase to β-phase (low temperature peak) and primary α-phase to β-phase (high temperature peak). Pederson et al.[15] reported that the phase fractions approach a constant value assumed to correspond to the equilibrium fraction. α→β transformation is relatively fast at all temperatures, having occurred after 10min, and near-constant phase content being reached within 30min. Most α+β→β transformations in α+β Ti-alloys develops via the increase of β-phase volume, because of migration of α/β interface.[13,18]

The study of the phase transformation kinetics during continuous cooling from β range is essential if the material is to be properly processed. DSC cooling curve of Ti-6Al-4V alloy from β range (1050˚C) at cooling rate 50˚C/min is shown in Figure 4b. At low cooling rates (50˚C/min), the diffusional transformation β→β+α occurs. By increasing the cooling rate using water quenching, it is possible to record dilatometric effects from the martensite reaction. Figure 5 shows the cooling curve of Ti-6Al-4V alloy, water quenched from 1050˚C (T_β+65˚C). The martensitic start temperature (Ms) varies depending on the starting structure and the homogeneity of the microstructure.[7] Ms temperature for the studied alloy is about 830°C (Figure 5). There is little information about the martensite transformation start and finish temperatures for Ti-6Al-4V alloy. It is reported[6] that martensite start temperature lies around 850°C for CP Ti. Venkatesh et al.[19] reported that β-phase was transformed into a stronger α'-phase after water quenching from above 800˚C. Malinov et al.[14] found that quenching Ti-6Al-4V alloy from 860°C resulted in a microstructure containing α+α' martensitic phase. Imam and Gilmore[18] reported that Ms temperature for Ti-6Al-4V alloy is higher than 843°C. Dąbrowski[9] determined Ms temperature using dilatometry to be 810˚C at 23.1˚C/sec cooling rate. On the other hand, several authors reported[5,18,20] that martensite transformation finish temperature (M_f) for Ti-6Al-4V alloy is below room temperature. Therefore, upon quenching not all β-phase is converted to α' martensite phase and small amount of β-phase retained after quenching to room temperature.[5]

Heat Treatment and Microstructure

Ti-6Al-4V α+β alloy is characterized to be sensitive to microstructural variations. Major microstructural parameters affecting mechanical properties of Ti-6Al-4V alloy are composition, size, volume fractions and morphology of α- and β-phases. [17, 18, 21, 22]

Microstructural Characteristics of Cast Ti-6Al-4V Alloy

Microstructure of the as-cast Ti-6Al-4V alloy is shown in Figure 6. The bright regions correspond to α-phase, forming a typical Widmansttaten structure, whereas thin dark regions between α-plates are β-phase.[5] Backscattered SEM image of the as-cast Ti-6Al-4V alloy is shown in Figure 7, here dark and light regions are α and β-phases, respectively. In the

Widmanstatten structure, α-phase is formed along prior β-grain boundaries, and colonies of lath-type β and α lamellar structure are present inside prior β grains. α and β platelets are known to have different Burgers direction.[6,7,21] It is reported[8] that the Widmanstatten α-phase can have several different morphologies. Slow cooling rates favor the formation of similarly aligned α-platelets in colonies, together with prior β-grain boundary α. Faster cooling rates favors more basketweave type of structure. Some authors consider the basketweave structure to be merely a finer form of Widmanstatten morphology,[5] whereas others[12] distinguish between the basketweave morphology and the Widmanstatten morphology, stating that, in the former the nucleation and growth of α-plates start not only from the β-grain boundaries but also within the β-grains.

X-ray diffraction pattern of the as-cast alloy is shown in Figure 8. Reflections of α and β phases were detected in diffraction patterns of the as-cast alloy. It should be noted that β reflections are rather weak, suggesting a relatively low volume fraction of the β-phase.[5] The volume fraction of β-phase was detected by XRD to be 10%. Malinov et al.[14] calculated the amount of retained β-phase from X-ray diffraction patterns to be 9±2% and reported that the amount of retained β-phase is independent on the cooling rate.

Effect of SSHT on Microstructure and Phase Transformation

The microstructures after different single stage heat treatments (SSHT) are shown in Figure 9. Water-quenching from the indicated temperatures in α+β range, and above Ms temperature according to our results shown in Figure 4 and Figure 5, leads to the formation of acicular α' martensite structure by diffusionless transformation of β-phase, as previously reported.[5-7,9,14,18] Optical micrographs of the alloy quenched from 900°C and 935°C are shown in Figures 9 (a-b), respectively. The microstructures formed in these conditions are a mixture of acicular α' martensite and β structures with α plates formed inside and at prior β-grain boundaries. α_P with more globular structure also begins to appear after quenching from α+β range along with α lamellar structure. The microstructure quenched from 935°C has higher fractions of α' martensite phase than quenched from 900°C. The optical micrograph of the alloy quenched from 980°C is shown in Figure 9c. Quenching from 980°C, just below Tβ, results in a microstructure that consists nearly of oriented-acicular α' martensite structure. Small bright areas of α-phase can be seen.

Backscattered SEM images (Figure 10) reveal the morphology of the acicular α' martensitic structure after SSHT from 935°C and 980°C. Morita et al[22] reported that the retained β-phase may be located in the lighted area around the α'-phase. In our study, the presence of the retained β-phase is detected around α'-phase after quenching as shown in Figure 11.

Many authors[5,18,22] pointed out that α-phase cannot be differentiated from α' martensite phase by X-ray diffraction measurements because the interplanar spacing in the two structures are nearly the same. Thereby, the obtained X-ray diffraction data can only confirm the presence of a stable β-phase in quantities high enough to be detected. X-ray diffraction patterns of the samples after SSHT are shown in Figure 12. The broadening and intensity of α+α' reflections, having high value of the full width at half maximum (FWHM), increase as the SSHT temperatures increase. This is an evidence for the presence of the supersaturated α' martensitic phase with hcp structure in increasing fractions as the SSHT temperature increases. These results are in agreement with previous data.[5,18,22]

The results of quantitative measurements of the volume fractions of the different phases after SSHT are presented in Figure 13. The volume fraction of α-phase was measured using an image analyzer, where α-phase appears bright in the optical micrograph and β- and α'-phases appear dark. β-phase volume fraction can be detected using XRD analysis; hence the volume fraction of α' martensite phase is a rough estimation, which equals to the supplement to 100%. As reported in Figure 13, the volume fraction of α-phase decreases with increasing SSHT temperature from 53% at 900˚C to 10% at 980˚C.

The presence of martensite in Ti-6Al-4V alloy has been widely reported.[1,3,5,9-11,18,22] Volume fraction of the martensite phase increases with increasing SSHT temperature, as presented in Figure 13. As the temperature increases, during heating, β-phase fraction increases at the expense of α-phase fraction and V becomes uniformly distributed in this β-phase. Therefore, the formed β-phase becomes leaner in β stabilizer (V%). If the β-phase is lean in β stabilizer when quenched, it is more likely to be unstable and transform to martensite.[8,18]

The presence of small amounts of the retained β-phase in the alloys upon quenching from α+β range is due to the fact that the martensite finish temperature, M_f, is below 25˚C for this alloy, as reported previously. Thus, upon quenching, not all β is converted to martensitic α'-phase.[5,18,20] As the temperature increases, during heating, the volume fraction of β-phase increases while its stability decreases; hence its M_f increases, and upon water quenching β-phase transforms to α' martensite and its retention decreases. In other words, β-phase formed at 980°C has the highest M_f while β-phase formed at 900°C has the lowest M_f in the studied SSHT temperature range. Therefore, the amount of retained β-phase at room temperature decreases as SSHT temperature increases, as presented in Figure 13.

Effect of DSHT on Microstructure and Phase Transformation

The morphology of α- and β-phases didn't change after DSHT, while their fraction and composition changed (Figure 14, Figure 15 and Figure 16.), as will be discussed below. Backscattered SEM images of the different microstructures after DSHT are shown in Figure 15. β-phase appears, here, as a bright regions. In these conditions, all the microstructures consist of parallel plates of α delineated by β-phase between them. There is no α' martensite phase formed after DSHT.

Figure 14 presents the volume fraction of α- and β-phases after DSHT. The microstructures after DSHT at 600°C had lower amount of retained β-phase than microstructures after DSHT at 700°C for all first stage temperatures. It is important to note that the volume fraction of retained β-phase decreases with increasing the quenching temperature, if the quenching temperature is higher than Ms temperature, as discussed in SSHT. This is attributed to that the occurring martensitic reaction consumes higher fraction of β-phase as the quenching temperature increases higher than Ms temperature, while, at lower quenching temperature, β-phase is retained at room temperature along with α-phase upon quenching.

During the controlled cooling step, i.e. furnace cooling, the diffusional β→α transformation takes place. α-phase first preferentially precipitates at the grain boundaries of the β-matrix. As the temperature drops, the side-plate α-phase grows from the grain boundary α-phase into the β-grains forming α-colony until they meet other α-colonies nucleated at other grain boundary areas of β-grain. The α-plates are separated within α-colonies by the retained β-phase.[6,7] The resulted microstructure is a Widmanstatten structure. As shown in Figure 4b, β→α+β transformation occurs at 870˚C during cooling. It is reported that[23] controlled cooling to lower temperatures was intended to promote the vanadium enrichment in β-phase by enhancing the

growth of α plates that enrich the β-phase with β stabilizers, through β→α+β transformation during slow cooling. The second isothermal step in the DSHT was intended to promote transformation of α+β→β which would initiate at α/β boundaries.

Holding at 600°C or 700°C will only permit the redistribution of the alloying elements due to diffusional process at these high temperatures. Quenching from these temperatures was resulted in microstructure free from brittle martensite phase. Water quenching from these temperatures also prevents the decomposition of β-phase. Hence higher amount of β-phase is retained to room temperature. As the temperature in the first stage increases, the amount of β-phase formed at this temperature increases through α+β→β transformation, as presented in the phase diagram of Ti-6Al and V shown in Figure 1, while furnace cooling from the first stage temperature leads to β→α+β transformation to take place. The kinetics of the transformation from the certain temperature in the first stage to 600˚C or 700˚C can be correlated to the volume fraction of α- and β-phases (Figure 14). It can be concluded that as the first stage temperature increases, the kinetics of the transformation increase, i.e. β→α+β transformation rate increases, that results in decreasing the fraction of β-phase with increasing the first stage temperature. For example, in the case of DSHT at 600˚C, volume fraction of β-phase is the highest after DSHT from 900˚C and lowest from 980˚C, while from 935˚C is intermediate value between them. Volume fraction after DSHT at 700˚C is changed in the same manner as at 600˚C.

As it is well known for Ti-6Al-4V α+β Ti-alloy that V is β-stabilizer that forms and enriches β-phase, while Al is α-stabilizer that forms and enriches α-phase. Since β-phase is the strengthening phase in these conditions, i.e. when the microstructure consists only from α- and β-phases, therefore, V content and distribution are the key factors that control the mechanical properties of the alloy. Figure 16 presented the chemical composition of both α- and β-phases after DSHT. α-phase is lean in V content (Figure 16a). As shown in Figure 16b, β-phase formed after DSHT at 600°C is richer in V content than that formed after DSHT at 700°C. Hence; β-phase formed after DSHT at 600°C is more stable. This can be illustrated by the fact that V concentration in the β-phase increases with decreasing its fraction as the second step treatment temperature decrease from 700˚C to 600˚C. This is accompanied with decreasing V content in α-phase and increasing its Al content.

On the other hand, for DSHT at 600˚C, the highest concentration of V content in β-phase is obtained from 900°C and the lowest from 980°C, while an intermediate value between them is obtained from 935°C. The concentration of V is changed in the same manner after DSHT at 700˚C from the same temperatures. This is in contradiction with the above fact, where the fraction of β-phase is not inversely proportional to its V content. This may be attributed to the increase in the V content of α-phase as the first step in the DSHT temperature increase from 900°C to 980°C. As presented in Figure 16, this increase in the V content in α-phase is accompanied with decreasing in its Al content.

It is reported[17] that upon furnace cooling from a predetermined temperature, the β-phase may decompose, depending upon its composition. The decomposition of the β-phase during the isothermal step of DSHT may also occur, again depending upon the β-phase composition. The decreased solubility of alloying element in β-phase during slow cooling induces precipitation of α-phase.[9] In our study, XRD was not detected any precipitates.

Finally, we can state that the phase transformation, i.e. fractions of the phases and their compositions, occur during DSHT is controlled mainly by V and Al diffusion. The decrease in the V content in β-phase is compensated by its increase in

the α-phase and the increase in V content is accompanied with decreasing in Al content in the same phase. This may be controlled by the diffusivity of V and Al in Ti.

Mechanical Properties

Tensile Properties

Effect of SSHT on Tensile Properties

Figure 17 shows the effect of SSHT temperature on the tensile properties, namely ultimate tensile strength, yield strength, elongation and ratio of YS/UTS, of Ti-6Al-4V alloy. As the SSHT temperature increases the tensile strength increases at the expense of tensile elongation. This is attributed to the increase in the amount of α' martensite phase as the SSHT temperature increases, as reported in Figure 13. Similar results were obtained by Venkatesh et al.[19] who stated that the effect of α' and α_p was the major contributor for these trends.

After SSHT at 900°C, tensile strength increases by 15.56% with a reduction in the elongation by 7.69% as compared with the as-cast alloy. On the other hand, the tensile strength increases by 24.4% and 25.6% with deterioration in elongation by 25.4% and 41% after SSHT at 935°C and 980°C, respectively, compared to the properties of the as-cast alloy.

Previous works[17,19] referred to the role that α_P plays in affecting the mechanical properties. The presence of α'- and α_p-phases decrease tensile elongation with an increase in tensile strength. This trend can be interpreted by their behavior under applied load, where α'- and α_p-phases act as crack initiators, that result in brittle fracture; hence low elongation. On the other hand, the reasons of enhancing strength that occurred due to the presence of α'- and α_p-phases are different. Rhodes et al.[17] reported that enhancing the yield strength due to the presence of α_p-phase can likely be traced to: (i) solid solution strengthening of β-phase. Since the hexagonal α-phase takes very little vanadium into solution; hence β-phase will be enriched with V as the volume fraction of α-phase increases with decreasing quenching temperature. (ii) α'-phase itself, on the other hand, is characterized with high strength. It is well known[5] that as the solution treatment temperature increases, α'-phase increases at the expense of α_p- and β-phases, and that tensile strength increases with reduction in elongation as the solution treatment temperature increases. This means that the effect of the presence and fraction of α' martensite phase is dominates and higher than the effect of α_p.

Figure 17 (b) presents the effect of SSHT temperature on the values of the ratio between the yield strength and tensile strength (YS/UTS). The ratio of YS/UTS increases with increasing the SSHT temperature from 900°C to 980°C. The lowest value of YS/UTS ratio means that tensile strength is higher enough than the yield strength, which gives chance for strain hardening transformation to occur, i.e. transformation of β-phase to stress induced martensite (SIM). The increase in the σ YS/UTS ratio with increasing temperature is attributed to lower volume fraction of retained β-phase as the SSHT temperature increases, as reported in Figure 13. Since β-phase is the responsible for the strain hardening phenomena, and its retention decreases with higher quenching temperature; hence the YS/UTS ratio increases. These results are in agreement with previous data.[5,18]

From these results we can say that the best temperature, for SSHT conditions, is 900°C, which is accompanied with the lowest YS/UTS ratio. At this temperature, there is good balance between the increase in the tensile strength and the reduction in the elongation as compared with the as-cast alloy.

Effect of DSHT on Tensile Properties

The effect of DSHT on the tensile properties of Ti-6Al-4V alloy is presented in Figure 18. The changes in the values of tensile strength and elongation are attributed to the change in the microstructure constituents after DSHT, especially the volume fraction and chemical composition of the present phases.

We need to consider the behavior of retained β-phase for explaining the change in the tensile properties after DSHT. As presented in Figure 18 (a), the ultimate tensile strength (UTS) increase and yield strength (YS) decreases after DSHT at 700°C as compared with those obtained at 600°C for all temperatures of the first step of the DSHT. The improvement in the ultimate tensile strength (UTS) after DSHT at 700°C over 600°C is due to higher volume fraction of β-phase at 700°C, as reported in Figure 14. The reduction in the value of yield strength (YS) after DSHT at 700°C compared with at 600°C can be attributed to increasing the V content in β-phase, with decreasing the temperature of the second step in DSHT (see Figure 16.b), that enhances the tensile yield strength of the alloy, as reported previously.[17] On the other hand, improvement in the elongation after DSHT at 600°C over 700°C can be attributed to the reduction in the amount of the strengthening β-phase, as reported in Figure 14.

The strengthening of metals is usually accompanied with a reduction in the ductility. However, after DSHT from 900˚C and 935˚C at 700˚C, both the elongation and strength of the alloy were improved over the as-cast alloy. This may be likely due to transformation induced plasticity (TRIP), enhanced by the strain-hardening due to the formation of strain-induced martensite (SIM) from the retained β-phase formed after quenching from 700°C. TRIP effect results in suppressing the plastic instability and extending the range of uniform elongation through two effects. First effect is transformation of retained β-phase during straining; and the second is the volume expansion that accompanied the transformation, as reported by Cooman for TRIP steels.[25] In our study, the strain-induced martensite transformation phenomena can be reflected through the change in the ratio of YS/UTS (Figure 18b), namely, this ratio was lowest after DSHT at 700°C condition and recovered with DSHT at 600°C. The lowest value of YS/UTS means that tensile strength is higher enough than the yield strength, that lets chance for strain hardening transformation to occur. Therefore, we can give a rational explanation that the recovery in the ratio of YS/UTS with decreasing the DSHT temperature was due to the reduction in the amount of retained β-phase and increasing its stability, i.e. its V content, as reported in Figure 14 and Figure 16. The stress-induced transformation of retained β-phase started at a relatively low applied stress level, this can be reflected by the decrease in the yield strength after DSHT at 700˚C, as reported in Figure 18.

The deterioration in the tensile properties after DSHT at 600˚C and 700˚C from 980˚C may be attributed to the decrease in the volume fraction of the retained β-phase, in addition to the decrease in the concentration of V in the retained β-phase, as reported in Figure 14 and Figure 18, i.e. decreasing the solid solution strengthening effect of β-phase.

From these results, it can be said that controlling the fraction and composition of retained β-phase are important factors in obtaining well-balanced microstructure of Ti-6Al-4V alloy. From this study, it can be concluded that the best DSHT cycle, that improves both tensile strength and elongation, is DSHT at 700˚C from 900˚C. This condition results in the highest ultimate tensile strength with lowest YS/UTS ratio and an increase in the elongation as compared with the as-cast alloy.

Impact Toughness and Fracture Behavior

Effect of SSHT on Impact Toughness

Figure 19 shows the effect of different SSHT temperatures on Charpy impact toughness. As shown, as the quenching temperatures increases, the Charpy impact toughness decreases. By reducing the volume fraction of martensitic α' phase from 80% at 980°C to 28% at 900°C, as reported in Figure 13, the impact toughness increases by 100%, namely from 5J to 10J. This may be accomplished using a lower solution temperature within (α+β) field. From Figure 19, it can be seen that the overall energy consumption is less for a larger volume fraction of martensitic. The impact toughness after SSHT deteriorates compared with as-cast alloy.

Effect of DSHT on Impact Toughness and Fracture Behavior

Charpy impact toughness values after DSHT are shown in Figure 20. Most of DSHT conditions achieve good values of energy consumption. This improvement in impact toughness is attributed to the formation of: (i) brittle martensite free microstructure after DSHT, and (ii) more homogenous structures upon the slow cooling step. After DSHT at 600°C, there is a considerable improvement in the impact toughness over at 700°C. This is attributed to the lower volume fraction of retained β-phase at 600°C, as reported in Figure 14. For this type of microstructure, a high Charpy impact toughness is explained by the strong deflection of the crack at the subcolonies of the lamellae packages.

Fractography

To exemplify the influence of crack deflection and the material's ductility on the Charpy impact behavior, SEM micrographs of the fractured specimens are shown in Figure 21. Fractograph of the as-cast specimen shows ductile fracture of dimple mode containing partly tiny cleavage type, giving mixed mode of fracture (Figure 21a). Widmanstatten has large colonies consisting of α-phase and strong β-phase, and these colonies have different lamellar directions. So severely crack branching and zigzaging are caused when cracks propagate, which increases resistance of crack propagation and bring out high impact toughness.[21]

The fracture surface of the alloy quenched from 900°C, Figure 21b, exhibited a dimple-like ductile fracture with lower amount of dimples compared with the as-cast structure (Figure 21a). In the alloy quenched from 980°C, Figure 21c, the fracture mode exhibited rough and smooth cleavage fracture surface with an increase in the cleavage size. After SSHT, therefore, the amount of dimples decreases and microcracks increase as compared with the as-cast structure while the dimples become finer (Figure 21). This may indicate that the primary α- and α' martensite phases play role in the fracture behavior.[19] This means that α' martensitic plates had a role of crack initiation sites and crack propagation, leading to clear cleavage fracture. α'-phase might provide an easy crack path or crack nucleation sites in a tensile overload failure. Thin martensitic α' plates will provide a poorer medium for energy absorption and limit resistance to crack propagation.[23]

Figure 22 presents the fracture surfaces of some selected specimens after DSHT. The alloy after DSHT from 900°C at 600°C exhibited a characteristic dimple-like ductile fracture with a large number of tear ridges, as shown in Figure 22a. Although the dimpled fracture surface of the DSHT condition from 935°C at 600°C (Figure 22b) looks rather ductile on the first sight, evidence for secondary cracking can be found, which indicates more brittle behavior when compared to Figure 22a.

On the other hand, the impact toughness values of the alloy after DSHT from 980°C at 600°C is the same of the as-cast condition but its fracture surface (Figure 22c) reveals more cleavage fracture with lower amount of dimples as compared with the as-cast specimen (Figure 21a). Besides many small dimples that characterize the fracture surfaces of the specimens after DSHT, also larger spallings can be found on the fracture surfaces, which originate from the crack travelling along lamellae interfaces. Comparing the fracture surface of the alloys after SSHT (Figure 21) and DSHT (Figure 22), it can be seen that the amount of microcracks decreased and became finer. This is attributed to the absence of the brittle martensite phase after DSHT.

CONCLUSIONS

The aim of this paper was to optimize the mechanical properties of Ti-6Al-4V castings through microstructure control via heat treatment. Different SSHT and DSHT cycles were conducted and the microstructure-properties relationship was established. The best heat treatment cycle that optimizes the mechanical properties of the alloy was determined. The following conclusions were drawn:

- Effect of SSHT on the microstructure-properties relationship:
  - α-, retained β- and α'-phases were observed in different combinations depending on the SSHT temperature.
  - SSHT improve tensile strength at the expense of elongation and impact toughness as compared with the as-cast condition. This is attributed to formation of α' acicular martensite phase upon quenching. This phase is brittle and initiates microcracks under dynamic load.
- Optimizing the mechanical properties was achieved after SSHT from 900°C as a result of obtaining a microstructure consisting of suitable fractions of the different phases, e.g. 53% soft α-, 19% retained β- and 28% hard α'-phases.
- Effect of DSHT on the microstructure-properties relationship:
  - α- along with retained β-phases, in different fractions and compositions, were formed after DSHT.
  - The main strengthening mechanism after DSHT is the solid solution strengthening of β-phase by V content.
  - DSHT (900°C-700°C) is selected as the best heat treatment that improves the combination between the properties as compared with as-cast condition. This is attributed to the characteristics of the formed microstructure that contains 20% retained β-phase with 9.58% V content whereas the as-cast microstructure contains 10% retained β-phase with 4.86% V content.
- The best heat treatment temperature should ensure the stability of β-phase; hence its retention at room temperature. The fraction and composition of the retained β-phase in the microstructure are the key factors to optimize the mechanical properties of Ti-6Al-4V alloy.
- The optimum the mechanical properties of Ti-6Al-4V castings can be achieved through a heat treatment cycle that results in formation of high fraction of metastable β-phase in the microstructure. The procedures of this heat treatment should include:

- Annealing at low temperature in α+β-range above Ms, e.g. 900˚C, to obtain high volume fraction of metastable β-phase by reducing transformation rate during the next step (furnace cooling).
- Permitting enrichment of β-phase by V through furnace cooling from this temperature to lower temperature, e.g. 700˚C.
- Water Quenching from the second step temperature to avoid decomposition of β-phase.

REFERENCES

1. L. W. Meyer, L. Krüger, K. Sommer, T. Halle and M. Hockauf, "Dynamic strength and failure behavior of titanium alloy Ti-6Al-4V for a variation of heat treatments", Mech. Time-Depend Mater, Vol. 12, PP: 237-247, (2008).
2. M. Bermingham, S. Mc Donald, M. Dargusch and D. Stjohn, "Microstructure of cast titanium alloys", Materials Forum, Vol. 31, PP: 84-89, (2007).
3. J. S. Tiley, "Modeling of microstructure property relationships in Ti-6Al-4V", Doctor of Philosophy Dissertation, Ohio State University, (2002).
4. R. R. Boyer, "An overview on the use of titanium in the aerospace industry", Materials Science and Engineering, Vol. A213, PP: 103-114, (1996).
5. M.T. Jovanovic, S. Tadic, S. Zec, Z. Miskovic and I. Bobic, "The effect of annealing temperatures and cooling rates on microstructure and mechanical properties of investment cast Ti-6Al-4V alloy", Materials and Design, Vol. 27, PP: 192-199, (2006).
6. G. Lütjering and J. C. Williams, "Titanium", 2nd edition, Springer, (2007).
7. C. Leyens and M. Peters, “Titanium and titanium alloys, fundamentals and applications”, WILEY-VCH Verlag GmbH & Co. KgaA, Weinheim, Germany, (2003).
8. R. Pederson, "Microstructure and phase transformation of Ti-6Al-4V", Licentiate Thesis, Lulea University of Technology, (2002).
9. R. Dąbrowski, "The kinetics of phase transformations during continuous cooling of the Ti6Al4V alloy from the single-phase β range", Archives of Metallurgy and Materials, Vol. 56, Issue 3, PP: 703-707, (2011).
10. H. Fujii, “Continuous cooling transformation characteristics of α+β Ti-alloys”, Nippon Steel Technical Report, No. 62, PP: 74-79, (1994).
11. T. Ahmed and H. J. Rack, “Phase transformations during cooling in α+β titanium alloys”, Materials Science and Engineering, Vol. A 243, PP: 206-211, (1998).
12. B. K. Damkroger and G. R. Edwards, “Continuous cooling transformation kinetics in alpha-beta titanium alloys”, Simulation and Theory of Evolving Microstructures, Metals & Materials Society, PP: 129-150, (1990).

13. W. Sha and Z. Guo, “Phase evaluation of Ti-6Al-4V during continuous heating”, Journal of Alloys and Compounds, Vol. 290, PP: L3-L7, (1999).
14. S. Malinov, Z. Guo, W.Sha and A. Wilson, "Differential scanning calorimetry study and computer modeling of β→α phase transformation in a Ti-6Al-4Valloy", Metallurgical and Materials Transactions A, Vol. 32 A, PP: 879-887, (2001).
15. R. Pederson, O. Babushkin, F. Skystedt and R. Warren, "The use of high temperature X-ray diffractometry to study phase transitions in Ti-6Al-4V alloy”, Institute of Materials, London, ISSN, PP: 1336-5510, (2001).
16. A. K. Shah, G. J. Kulkarni, V. Gopinathan and R. Kiushnan, "Determination of activation energy for α+β→β transformation in Ti-6AI-4V alloy by dilatometry", Scripta Metallurgica et Matekdia, Vol. 32, No. 9, PP: 1353-1356, (1995).
17. C. Rhodes and N. Paton, "The influence of α/β interface phase on tensile properties of Ti-6AI-4V", Metallurgical Transactions, Vol. 10 A, PP: 1753-1758, (1979).
18. M. Imam and C. Gilmore, "Fatigue and microstructural properties of quenched Ti-6AI-4V", Metallurgical Transactions, Vol. 14 A, PP: 233-240, (1983).
19. B. D. Venkatesh, D. L. Chen and S. D. Bhole, "Effect of heat treatment on mechanical properties of Ti-6Al-4V ELI alloy", Materials Science and Engineering, Vol. A 506, PP: 117-124, (2009).
20. M. E. Ramosoeu, H. K. Chikwanda, A. S. Bolokang, G. Booysen and T. N. Ngonda, "Additive manufacturing: characterization of Ti-6Al-4V alloy intended for biomedical application", The Southern African Institute of Mining and Metallurgy- Advanced Metals Initiative- Light Metals Conference, PP: 337-344, (2010).
21. D. G. Lee, S. Lee and Y. Lee, "Effect of precipitates on damping capacity and mechanical properties of Ti–6Al–4V alloy", Materials Science and Engineering, Vol. A, No. 486, PP: 19-26, (2008).
22. T. Morita, K. Hatsuoka, T. Iizuka and K. Kawasaki, "Strengthening of Ti-6Al-4V alloy by short-time duplex heat treatment", Materials Transactions, Vol. 46, No. 7, PP: 1681-1686, (2005).
23. K. C. Yung, B. Ralph, W.B. Lee and R. Fenn, "An investigation into welding parameters affecting the tensile properties of titanium welds", Journal of Materials Processing Technology, Vol. 63, PP: 759-764, (1997).
24. White Paper. Sub-zero treatment, technology, processes and equipment, linde Group, Germany, (2010).
25. B. C. De Cooman, “Structure-properties relationship in TRIP steels containing carbide-free bainite”, Solid State and Materials Science, Vol. 8, PP: 285-303, (2004).

APPENDICES

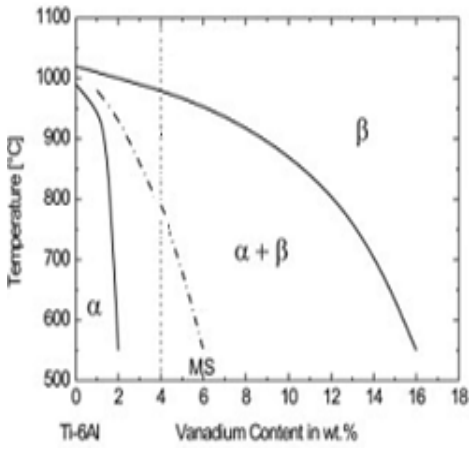

Figure 1: Phase Diagram of Ti-6Al-4V Alloy[3,5]

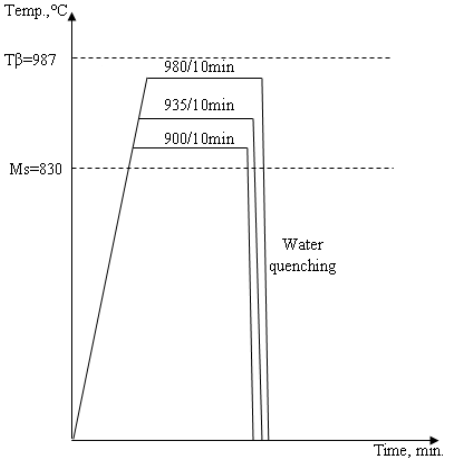

Figure 2: Schematic Drawing of SSHT Cycles

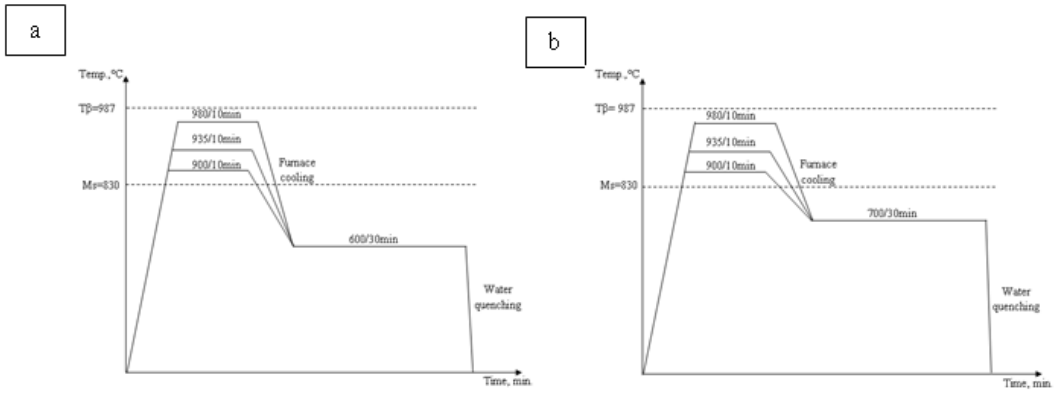

Figure 3: Schematic Drawing of DSHT Cycles at Different Temperatures: (a) 600°C and (b) 700°C

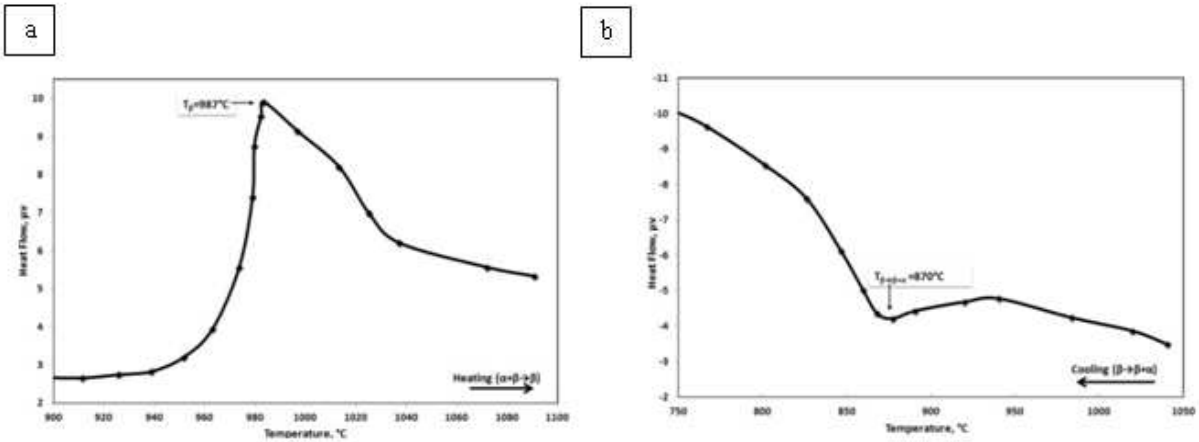

Figure 4: DSC Results for Ti-6Al-4V Alloy: (a) Heating and (b) Cooling Curves

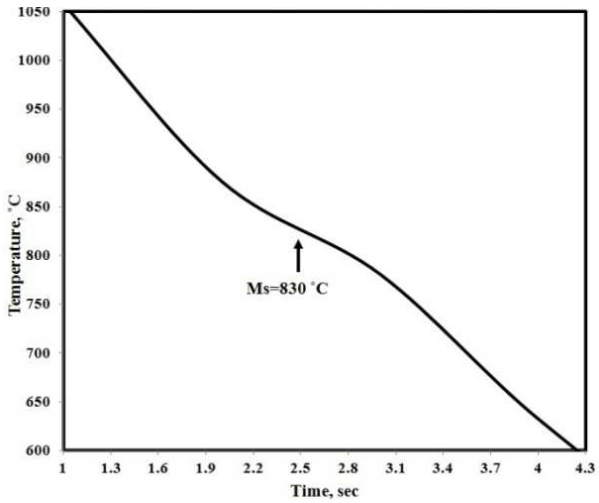

Figure 5: The Cooling Curve of Ti-6Al-4V Alloy Water Quenched from 1050˚C

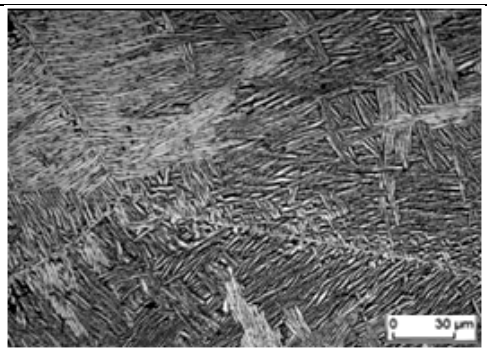

Figure 6. Microstructure of the Ascast Ti-6Al-4V Alloy Shows Widmanstta-ten Structure, thin Dark Regions between α-plates are β-phase.

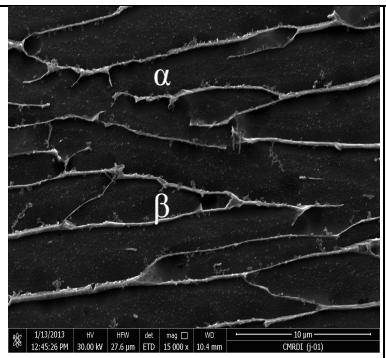

Figure 7. Backscattered SEM image of the as-cast Ti-6Al-4V alloy. Dark and light Regions are α and β-phases, Respectively.

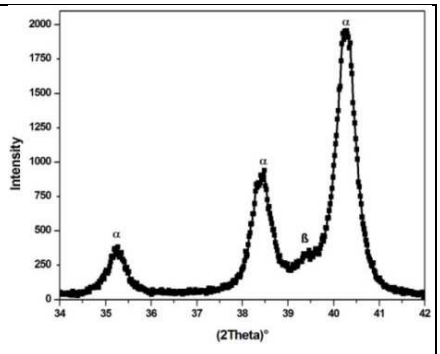

Figure 8: X-Ray Diffraction Patterns of the As-Cast Ti-6Al-4V Alloy

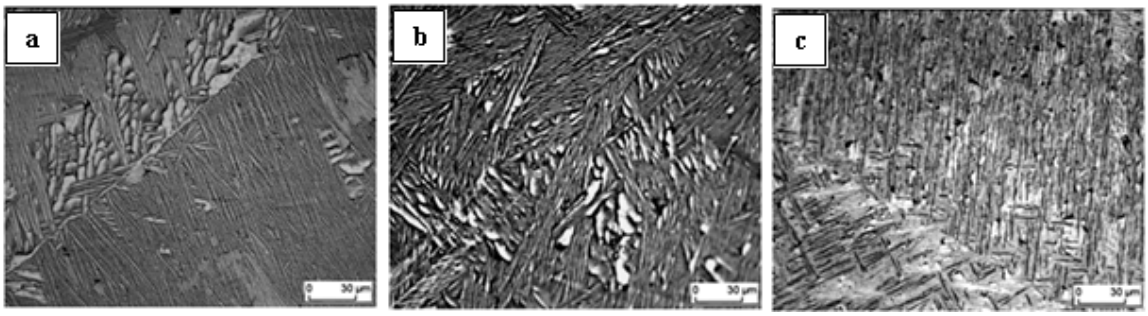

Figure 9: Optical Micrographs of the Microstructure after SSHT from: (a) 900°C; (b) 935°C and (c) 980°C

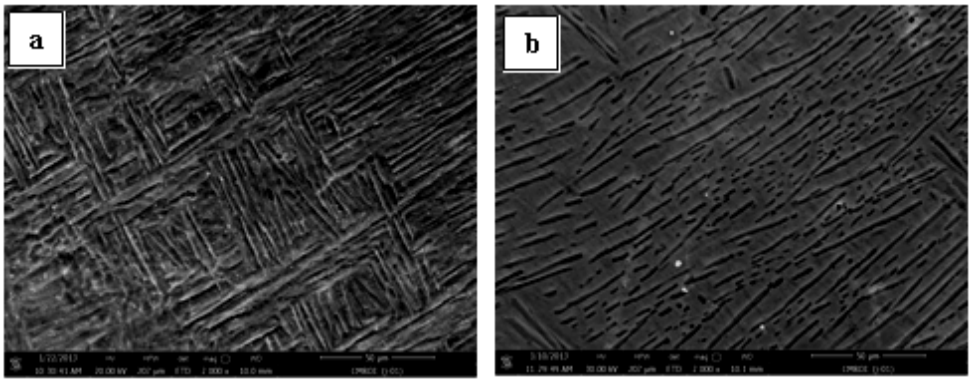

Figure 10: Backscattered SEM Images Show the Morphology of the Formed Acicular α' Martensitic Structure after SSHT from: (a) 935°C and (b) 980°C

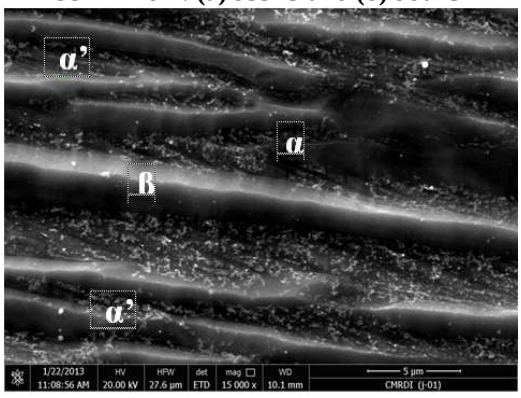

Figure 11: Backscatter SEM Image Shows the Presence of β-Phase in Lighted Areas around Martensite Lath after SSHT from 935˚C

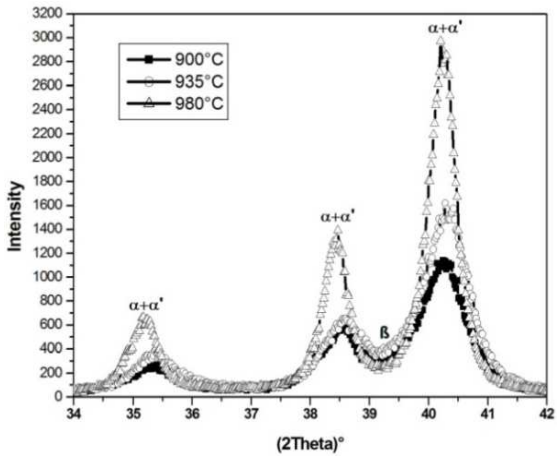

Figure 12: X-Ray Diffraction Patterns after SSHT from Different Temperatures

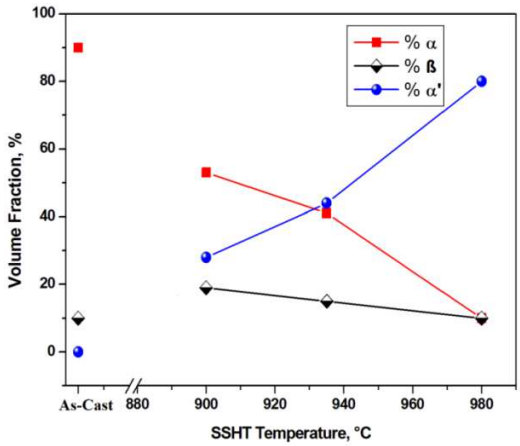

Figure 13: Volume Fraction (%) of the Present Phases after SSHT

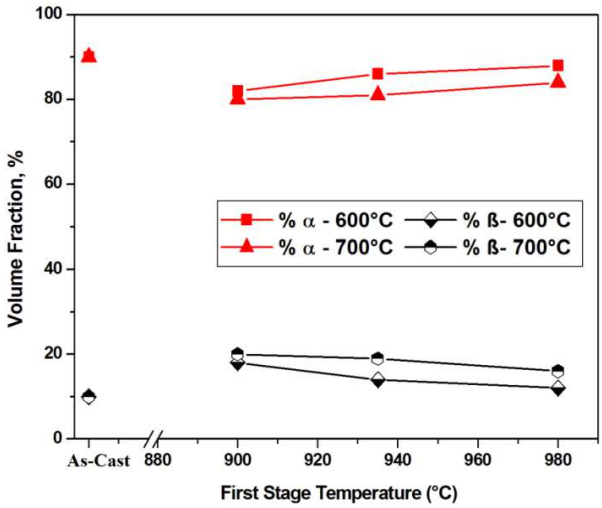

Figure 14: Volume Fraction (%) of the Present Phases after DSHT

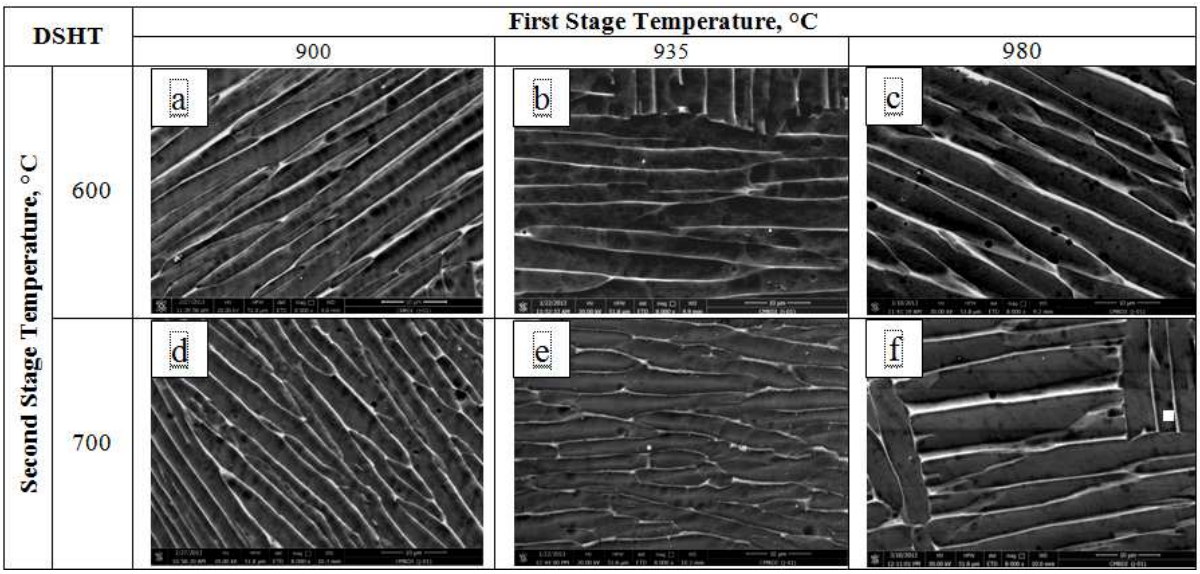

Figure 15: Backscattered SEM Images of Ti-6A1-4V Alloy after Different First and Second Stage Temperatures of DSHT

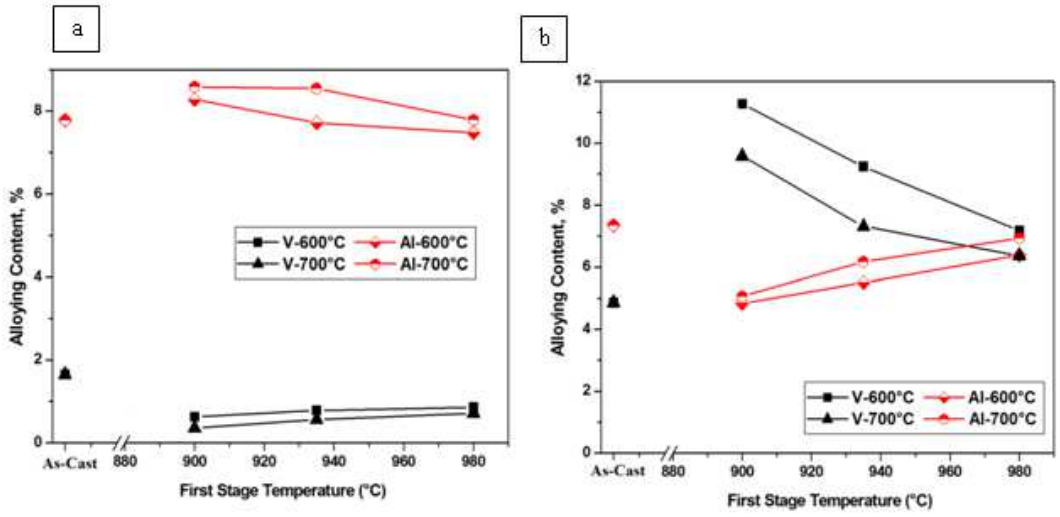

Figure 16: Alloying Contents (%) in α- and β- Phases after DSHT: (a) α- and (b) β-Phases

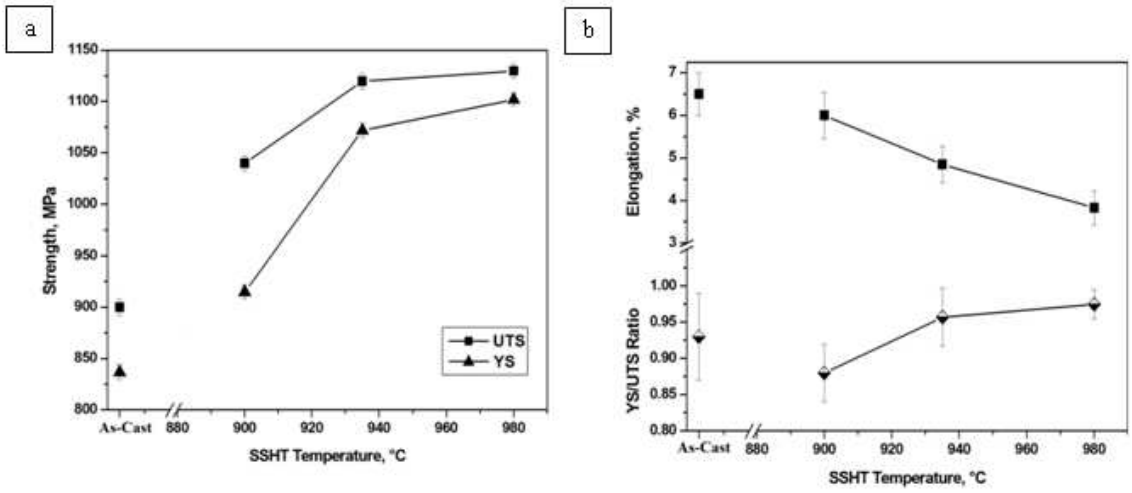

Figure 17: Effect of Different SSHT Temperatures on Tensile Properties: (a) Strength and (b) Elongation and the Ratio of σ_{YS}/σ_{UTS}

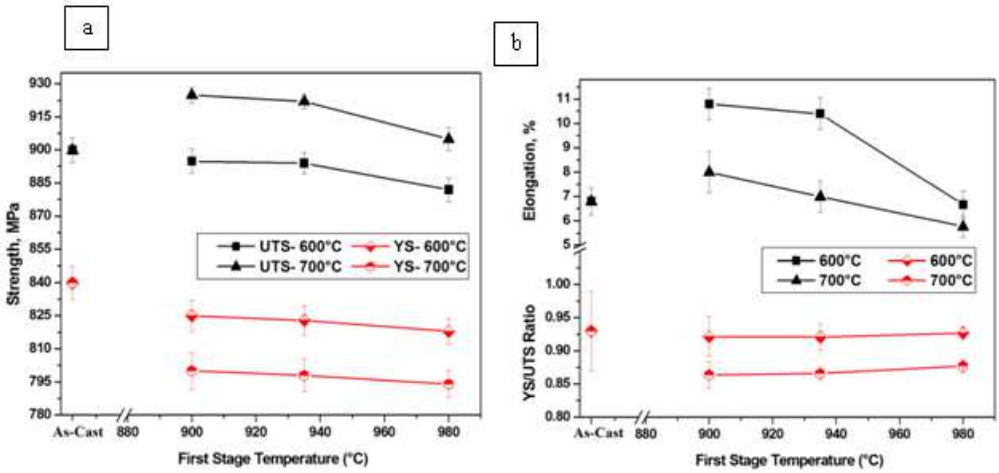

Figure 18: Effect of Different DSHT on Tensile Properties: (a) Strength and (b) Elongation and the Ratio of σ_{YS}/σ_{TS}

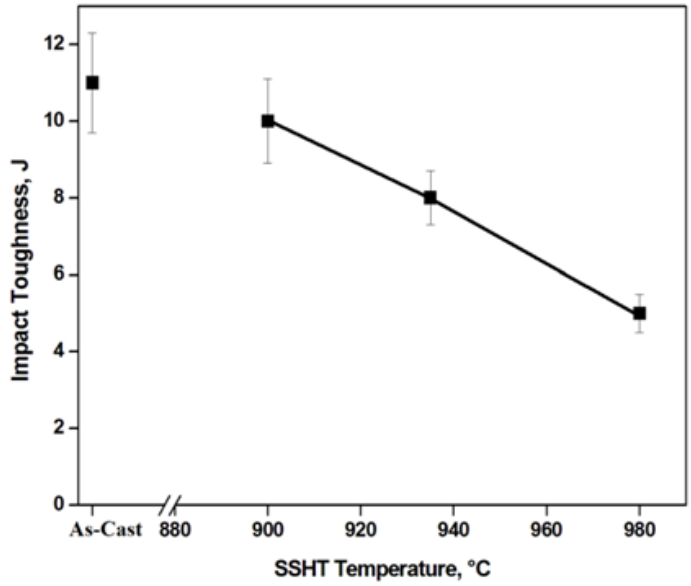

Figure 19: The Effect of Different SSHT Temperatures on Charpy Impact Toughness

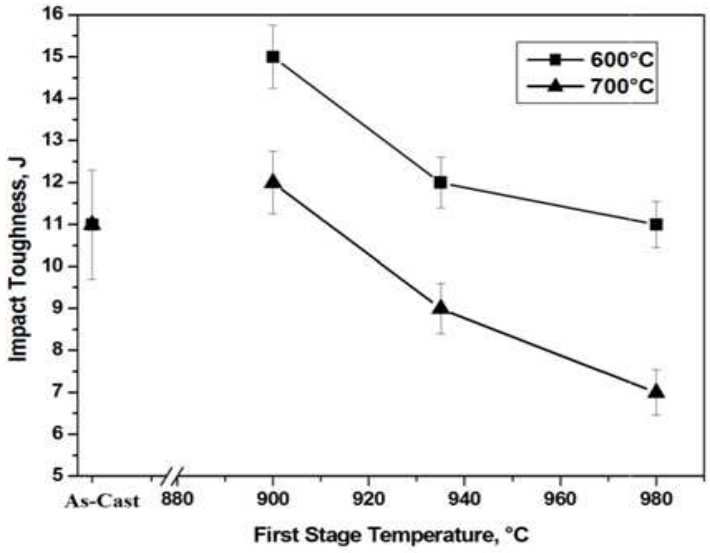

Figure 20: Effect of DSHT on Energy Consumption in Charpy Impact Test

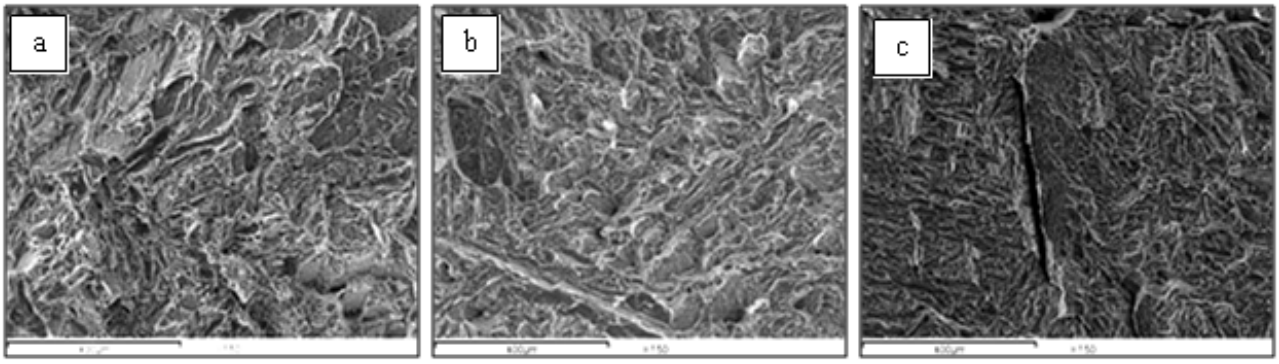

Figure 21: SEM Fractographs of Charpy Impact Specimens: (a) As-Cast, (b) SSHT at 900°C, and (c) SSHT at 980°C

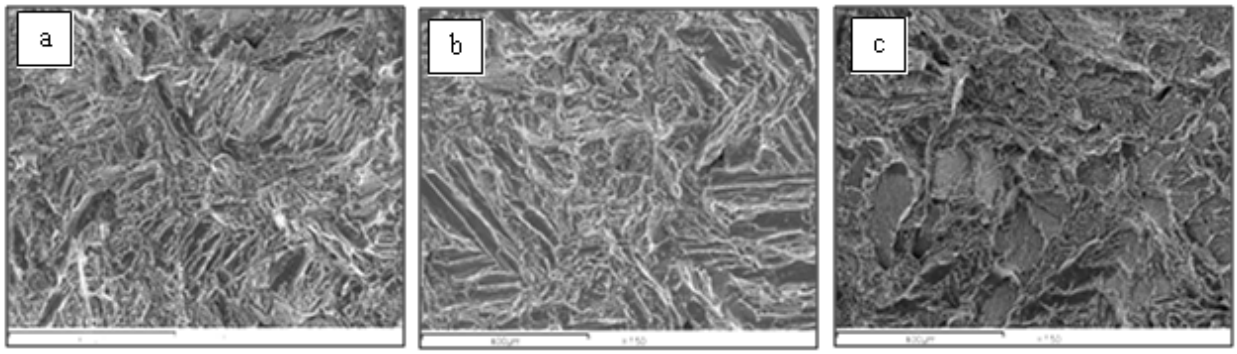

Figure 22: SEM Fractographs of Charpy Impact Specimens after DSHT: (a) 900°C-600°C, (b) 935°C-600°C, and (c) 980°C-600°C